Benchmark Test of a Finite Element Solver for Compressible Flows

o   Yang GUO, I.I.S., The University of Tokyo, 4-6-1 Komaba, Meguro-ku, Tokyo 153-8505, guoyang@iis.u-tokyo.ac.jp

Chisachi KATO, I.I.S., The University of Tokyo, 4-6-1 Komaba, Meguro-ku, Tokyo 153-8505, ckato@iis.u-tokyo.ac.jp

Yoshinobu YAMADE, Mizuho Information & Research Institute, Inc., 2-3 Kanda Nishikicho, Chiyoda-ku, Tokyo 101-0054, yyamade@iis.u-tokyo.ac.jp

Abstract   A compressible flow solver using the finite element method was developed. Three benchmark test cases were validated: a simple acoustic problem in a cavity, laminar flow around a square cylinder and turbulent flow around a NACA0012 airfoil. In the simple acoustic problem in the cavity, the time history of sound pressure at a sampling point agrees well with the theoretical solution. In the laminar flow around a square cylinder, the normalized r.m.s. pressure along a sampling line agrees reasonably well with the theoretical solution. In the turbulent flow around NACA0012 airfoil, the mean pressure coefficient, r.m.s. pressure coefficient and the mean velocity profiles in the turbulent boundary layer agree fairly well with the experimental one.

1. Introduction

Although incompressible flow solver is popular when computing low-Mach-number (M<0.3) flow, there are situations that requires compressible flow solver. One of these is direct simulation of sound generated from the flow, where the flow field and acoustic field are computed at the same time. On the other hand, if the Mach number is larger than 0.3, the compressible effects must be considered. Thus developing a compressible flow solver will be helpful to extend the application range of a CFD package.

The Finite Element Method (FEM) has great capability to handle complicated flow geometries often encountered in the real-world problems. Thus it is adopted for the spatial discretization. The purpose of the paper is to validate the accuracy of the developed finite element solver for compressible flows.

2. Computational methods

The governing equations of compressible flows for a perfect gas are the followings:

Continuity equation:

$$\frac{\partial \rho}{\partial t} + \frac{\partial (\rho u_j)}{\partial x_j} = 0 \tag{1}$$

Momentum equations:

$$\frac{\partial (\rho u_i)}{\partial t} + \frac{\partial (u_j \rho u_i)}{\partial x_j} = -\frac{\partial p}{\partial x_i} + \frac{\partial}{\partial x_j}\left[\mu\left(\frac{\partial u_i}{\partial x_j}+\frac{\partial u_j}{\partial x_i}\right)\right] - \frac{\partial}{\partial x_i}\left(\frac{2}{3}\mu\frac{\partial u_j}{\partial x_j}\right) \tag{2}$$

Energy equation:

$$\frac{\partial (\rho e)}{\partial t} + \frac{\partial (u_j \rho e)}{\partial x_j} = -p\frac{\partial u_j}{\partial x_j} + \frac{\partial}{\partial x_j}\left(K\frac{\partial T}{\partial x_j}\right) + 2\mu S_{ij}S_{ij} - \frac{2}{3}\mu\left(\frac{\partial u_j}{\partial x_j}\right)^2 \tag{3}$$

Equation of state:

$$p = \rho R T \tag{4}$$

where ρ is the density, u_i(i=1,2,3) are the velocity components, p is the pressure and T is the temperature. e is the internal energy per unit mass calculated by $e = c_v T$, where c_v is the specific heat capacity at constant volume calculated by $c_v = \frac{1}{\gamma-1}R$, where γ is the heat capacity ratio and R is the gas constant. μ is the dynamic viscosity and K is the heat conduct coefficient. S_{ij} (i=1,2,3 and j=1,2,3) are the components of strain rate tensor.

In the low-Mach-number (M<0.3) flow, we can use the isentropic assumption,

$$\frac{Dp}{D\rho} = c^2 \tag{5}$$

where c is the speed of sound. The assumption is valid if adiabatic condition is satisfied and the change of density and temperature is small. In this case, the energy equation is not solved.

FEM with standard Galerkin is used for the spatial discretization. The Euler forward scheme is used for time discretization of continuity equation. The Crank-Nicolson scheme is used for time discretization of momentum equations and energy equation. The resulting second-order numerical scheme has no numerical dissipation but has phase error which depends on the time increment and the mesh resolution.

3. Computational results

3.1 3D simple acoustic problem

The computational model of 3D simple acoustic problem without flow is shown in Fig. 1. The computational domain is a cavity of 1 m × 1 m × 1 m. This problem is originally from the Benchmark Platform on Computational Methods for Architectural/Environmental Acoustics[1]. However, the initial condition was changed from an initial impulse to an initial condition with finite frequency range (8 wave components in each direction) as the following:

$$p = \sum_{k_1=1}^{8}\sum_{k_2=1}^{8}\sum_{k_3=1}^{8}\cos\left(k_1\pi x\right)\cos\left(k_2\pi y\right)\cos\left(k_3\pi z\right) \tag{6}$$

$$\frac{\partial p}{\partial t} = 0$$

The hard wall boundary condition was imposed on the

boundaries. A hexahedral mesh with 160^3 uniform distributed elements was used in the computation. The sound speed is set to c_0 =343.0 m/s. The minimum grid points per wavelength (PPW) is about 23. The time increment is set to Δt = 1.25×10^{-5} s (CFL≈ 0.7).

The theoretical solution of the acoustic problem is as the following:

$$p = \sum_{k_1=1}^{8}\sum_{k_2=1}^{8}\sum_{k_3=1}^{8} \cos(k_1 \pi x)\cos(k_2 \pi y)\cos(k_3 \pi z) \tag{7}$$
$$\bullet \cos\left(\sqrt{k_1^2 + k_2^2 + k_3^2}\,\pi c_0 t\right)$$

The computed sound pressure at a sampling point that is at the corner of (1 m, 1 m, 0 m) is compared with the theoretical solution. The computed result shown in Fig. 2 agrees well with the theoretical solution in terms of amplitude and phase up to t = 0.04 s, until which the acoustic wave propagated in the cavity and was reflected by the wall for about 12 times. This demonstrates that the current numerical schemes can predict the propagation of the sound wave with enough accuracy if appropriate parameters are selected.
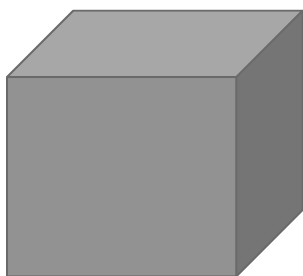

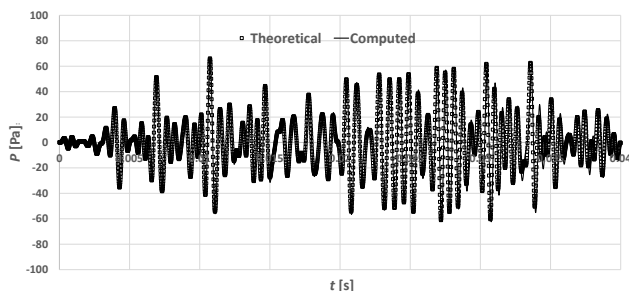Fig. 1　Computational model of 3D benchmark: acoustic problem in a cavity (1 m × 1 m × 1 m)

Fig. 2　Comparison of time history of sound pressure at the corner of (1 m, 1 m, 0 m)

3.2 Laminar flow around a square cylinder

Laminar flow around a square cylinder was computed. The Reynolds number based on inlet velocity (U_0) and the side length (D) of the square cylinder is 150. The Mach number is set to 0.2. The computation is essentially two-dimensional. The size of the computational domain is 1000D × 1000D. The number of total mesh points is about 27 million. The minimum PPW for dominating sound wave is 32. The first order non-reflecting boundary condition was used in the far-field boundaries.

Figure 3 shows the U-component of the velocity field. It is confirmed the distribution of mean U-component of the velocity

along y=0 line agrees reasonably well with that of Yokoyama and Iida[2], which is computed by a sixth-order compact scheme.

The distribution of instantaneous non-dimensional pressure is shown in Fig. 4. The pressure at the far-field represents the acoustic field and propagation of acoustic wave is clear.

Figure 5 compares the normalized r.m.s. pressure at x=0.5 line, where the theoretical value is obtained by assuming the sound pressure decays with the square root of the distance. The computed value agrees fairly well with the theoretical one. Some overprediction of r.m.s. pressure is observed around r/D=30. We assume that this is due to the effects of some reflection of pressure wave at the inlet and the breakdown of vortices at about 200D downstream from the cylinder.
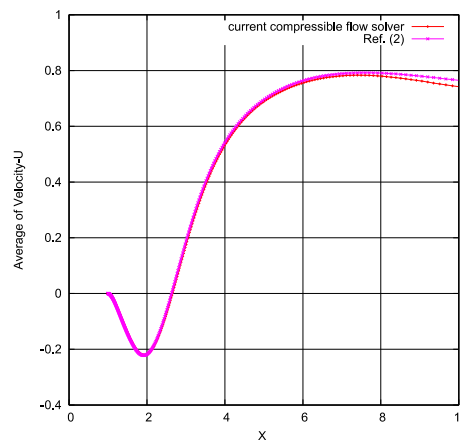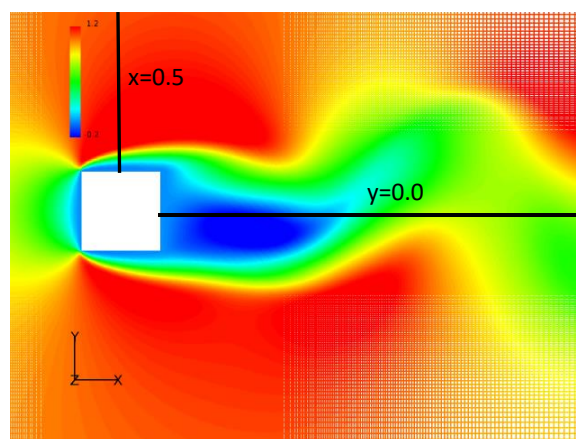

Fig. 3　Velocity field computed by the compressible solver (top: distribution of velocity, bottom: comparison of velocity profile between FFB and data from the reference paper (2) at y=0 line)
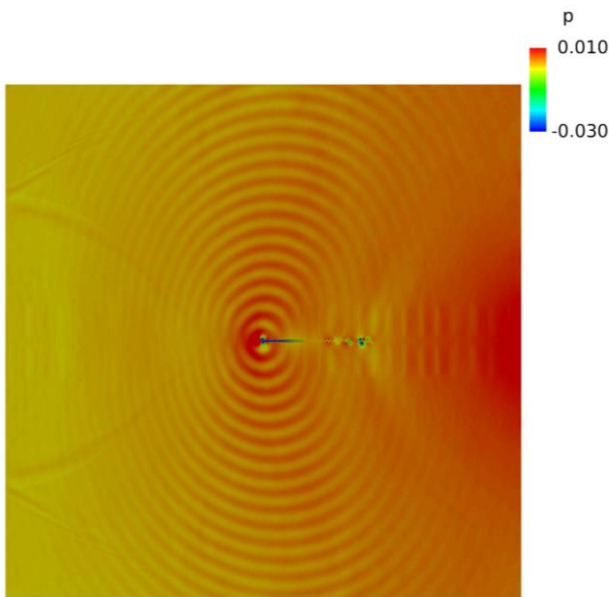
Fig. 4   Instantaneous non-dimensional pressure field computed by the compressible solver
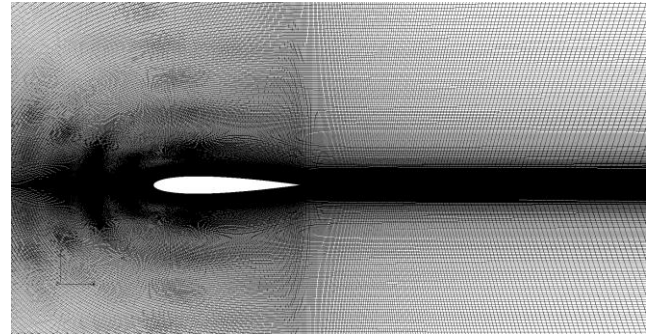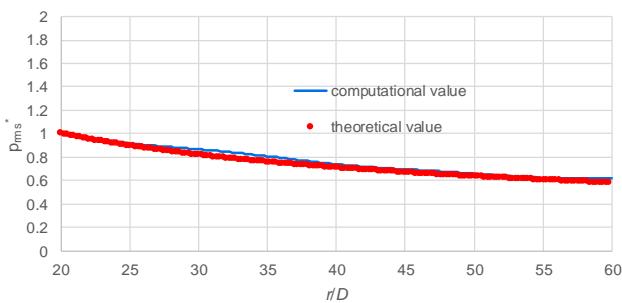

Fig. 5   Comparison of normalized r.m.s. pressure at x=0.5 line

3.3 Turbulent flow around a NACA0012 airfoil

Turbulent flow around a 2D NACA0012 airfoil was calculated by large-eddy simulation (LES). The Reynolds number based on inlet velocity (U) and the chord length (C) of the airfoil is 2×10^5. The angle of attack is 9 degrees. The Mach number is set to 0.3, which is higher than the actual Mach number. We set this Mach number to avoid the numerical stiffness and assume that the Mach number of 0.3 does not change the flow field essentially.

The size of computational domain in xy plane is $40C$ and the spanwise length is $0.05C$. The mesh sizes in the turbulent boundary layer (TBL) with wall units are Δx^+=45, Δy^+_{min}=2, Δz^+=25. The mesh near the airfoil is shown in Fig. 6. The number of total mesh points is about 13 million. Dynamic Smagorinsky Model (DSM)[3] with modification by Lilly[4] are implemented to account for the effects of subgrid-scale (SGS) stresses.

The vortical structures are represented by instantaneous iso-surface of Laplacian of normalized pressure, which is shown in Fig. 7. At about 3% of the chord length from the leading edge, there is a short laminar separation bubble and the flow transition happens after the bubble. Streamwise vortical structures can be seen after the transition finishes.

The comparison of computed pressure coefficient on the airfoil and the experimental value of Miyazawa et al.[5] is made in Fig. 8. The overall agreement of mean pressure coefficient and r.m.s.

pressure coefficient on the airfoil surface is good, except that near the leading edge the computed r.m.s. pressure coefficient shows some oscillation and the value is somewhat overpredicted.

Comparison of the velocity profiles in TBL is shown in Fig. 9 and Fig. 10. The overall agreement of mean velocity profile and r.m.s. velocity profile at x/C=0.5 and x/C=0.7 is good. But the mean velocity is slightly underpredicted and r.m.s velocity is somewhat overpredicted. We assume the reason is that the mesh resolution is still not fine enough to fully resolve the TBL.
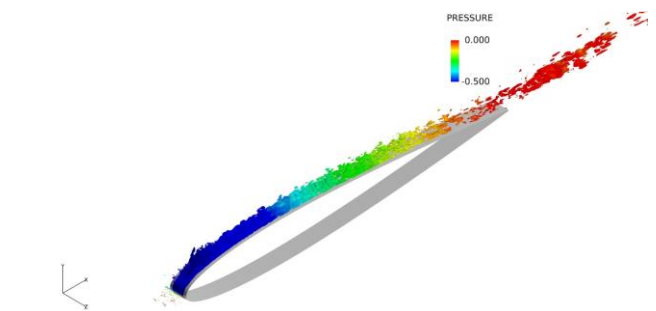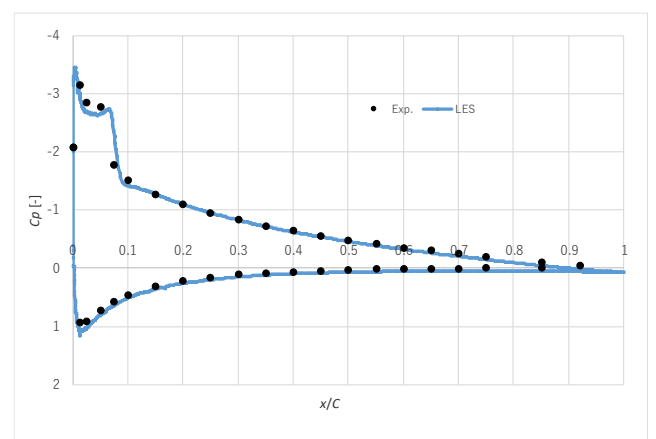

Fig. 6 Mesh near the NACA0012 airfoil

Fig. 7   Instantaneous iso-surface of Laplacian of normalized pressure (Color represents normalized pressure)
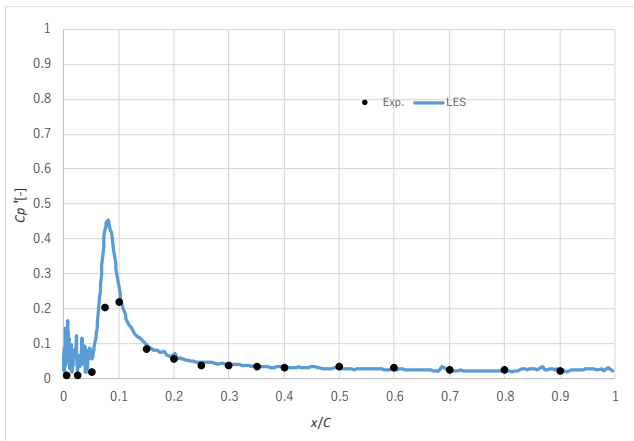

3

Fig. 8   Mean pressure coefficient (top) and r.m.s. pressure coefficient (bottom) on the airfoil surface
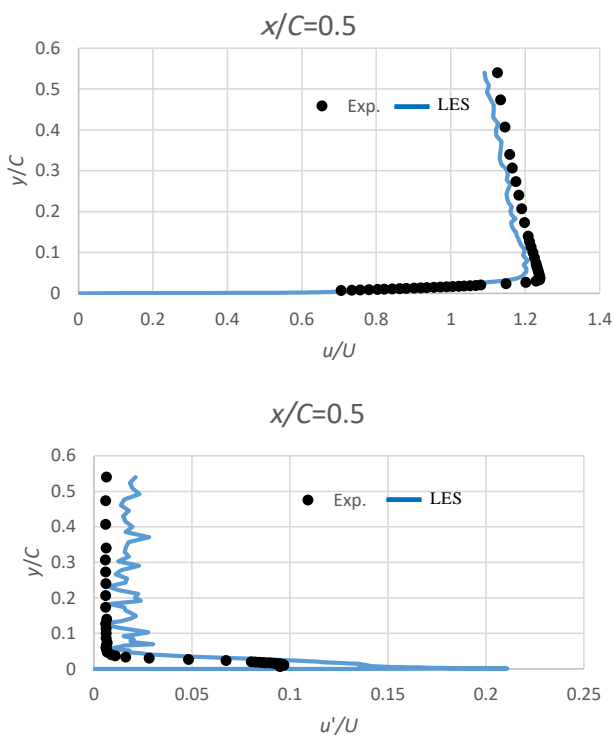

Fig. 9   Mean velocity profile (top) and r.m.s. velocity profile (bottom) at x/C=0.5 on the suction side of airfoil surface
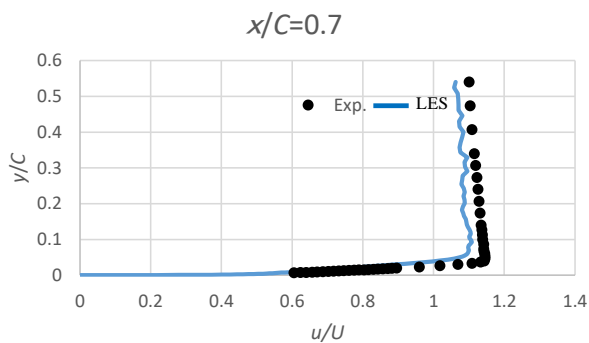

Fig. 10   Mean velocity profile (top) and r.m.s. velocity profile (bottom) at x/C=0.7 on the suction side of airfoil surface

4. Discussion and Conclusions

Three benchmark test cases were computed to validate the accuracy of the developed compressible FEM flow solver: a simple acoustic problem in the cavity, laminar flow around a square cylinder and turbulent flow around a NACA0012 airfoil. The overall agreement of computed flow field or acoustic field and the experimental results or theoretical one is good. The validation of accuracy of sound prediction in turbulent flow will be the work in the next stage.

Bibliography

(1)   http://gacoust.hwe.oita-u.ac.jp/aij-bpca/B0-1T/index.html.
(2)   Yokoyama, H. and Iida, A., "Aerodynamic Sound Sources from Flows around a Rectangular Cylinder with a Low Mach Number," Transactions of the Japan Society of Mechanical Engineers. B (in Japanese), Vol. 79, No. 799 (2003), pp. 344-355.
(3)   Germano, M., et al., "A Dynamic Subgrid-Scale Eddy Viscosity Model," Phys. Fluids A, Vol. 3, No. 7 (1991), pp. 1760-1765.
(4)   Lilly, D. K., "A Proposed Modification of the Germano Subgrid-Scale Closure Method," Phys. Fluids A, Vol. 4, No. 3 (1992), pp. 633-635.
(5)   Miyazawa, M., Kato, C., Suzuki, Y., Takaishi, T., "Aeroacoustic Simulation of a Flow around a 2-D Aerofoil: 1st Report, Validation of a Large Eddy Simulation of Separated and Transitional Flow around an Aerofoil," Transactions of the Japan Society of Mechanical Engineers. B (in Japanese), Vol. 72, No. 721 (2006), pp. 2140-2147.